SiH_2Cl_2: *Ab initio* anharmonic force field, dipole moments, and infrared vibrational transitions

An-Wen Liu
Hefei National Laboratory for Physical Sciences at Microscale, Department of Chemical Physics, University of Science and Technology of China, Hefei, 230026, China

Shui-Ming Hu[a)]
Hefei National Laboratory for Physical Sciences at Microscale, Department of Chemical Physics, University of Science and Technology of China, Hefei, 230026, China and Shanghai Institute for Advanced Studies, University of Science and Technology of China, Shanghai, 201315, China

Qing-Shi Zhu
Hefei National Laboratory for Physical Sciences at Microscale, Department of Chemical Physics, University of Science and Technology of China, Hefei, 230026, China

(Received 1 July 2005; accepted 6 September 2005; published online 28 October 2005)

The vibrational spectra of SiH_2Cl_2 have been recorded in the 1000–13 000 cm^{-1} region, utilizing the Fourier-transform spectroscopy and Fourier-transform intracavity laser absorption spectroscopy. Totally 61 band centers and intensities are derived from the infrared spectra. An *ab initio* quartic force field is obtained by applying the second-order Møller-Plesset perturbation theory and correlation-consistent polarized valence triplet-zeta basis sets [J. Chem. Phys. **90**, 1007 (1989); **98**, 1358 (1993)]. Most observed bands are assigned by the vibration analysis based on the second-order perturbation theory. Reduced-dimensional *ab initio* dipole moment functions (two dimensional and three dimensional) have also been calculated to investigate the absolute band intensities of the SiH_2 chromophore. The calculated values agree reasonably with the observed ones. © *2005 American Institute of Physics*. [DOI: 10.1063/1.2090267]

I. INTRODUCTION

The chlorinated silanes, particularly dichlorosilane and trichlorosilane, attract interests in many applications because they are used as precursors for the chemical-vapor deposition of epitaxial silicon. They also attract fundamental interests in the study of the local-mode nature of the Si–H chromophore. The vibrational transitions of $SiHCl_3$ were studied earlier[1–3] and recently.[4] He *et al.* carried out *ab initio* calculations on reduced-dimensional potential-energy and dipole moment surfaces.[5] Zheng *et al.* gave an *ab initio* anharmonic force field, which can reproduce most of the observed vibrational transitions.[6] Dichlorosilane SiH_2Cl_2 were studied earlier in the fundamentals[7–9] and from the fifth through eighth Si–H stretching overtones.[2] Due to the lack of high-resolution spectroscopic data, the anharmonic constants and harmonic frequencies have not been obtained yet.

In recent years, much progress has been achieved in the predictions of molecular properties based on accurate *ab initio* potential-energy surface. Meanwhile, a high-quality anharmonic force field can be very instructive in the studies of rovibrational spectroscopy and thermodynamic and dynamic properties of small molecules. The method of using the second-order Møller-Plesset (MP2) perturbation theory[10] to get a full-dimensional *ab initio* potential-energy surface up to the fourth-order force constants has been successfully applied to derive the anharmonic force fields of some halide silanes: $SiHF_3$,[11] $SiHCl_3$,[6] and SiH_2F_2.[12] Here we will present vibrational analysis of the dichlorosilane molecule from infrared-absorption spectroscopy and *ab initio* calculations. Experimental details to get the band centers and absolute band intensities of SiH_2Cl_2 are given in Sec. II. The anharmonic force field study and band assignments will be presented in Sec. III. Reduced-dimensional [two-dimensional (2D) and three-dimensional (3D)] *ab initio* dipole moment functions and the comparison between calculated and observed band intensities will be given in Sec. IV. The results will be summarized in Sec. V.

II. EXPERIMENTAL DETAILS

The dichlorosilane sample was purchased from Nanjing Special Gas Company (China) and the stated purity is 98%. The absorption spectra in the 1000–9000 cm^{-1} region were recorded with a Bruker IFS 120HR Fourier-transform spectrometer with a resolution of 0.2 cm^{-1} at room temperature (293±1 K). Because of the wide spectral range and the large variation of the absorption line intensities, the Fourier-transform (FT) spectra were recorded under several different experimental conditions which are listed in Table I. Some bands recorded by Fourier-transform spectroscopy (FTS) are illustrated in Fig. 1.

Fourier-transform intracavity laser absorption spectroscopy (FT-ICLAS) integrates the high-sensitivity advantage of ICLAS and the high-resolution and the high-precision advantage of FTS. It is very suitable to the quantitative mea-

[a)]Author to whom correspondence should be addressed. Fax: +86-551-3602969. Electronic mail: smhu@ustc.edu.cn

TABLE I. Experimental conditions used to record the absorption spectrum of SiH_2Cl_2.

Region (cm^{-1})	Pressure (Pa)	Detector	Path length (m)	Beam splitter	Source
1000–5000	151	MCT	33	KBr	Globar
1500–3000	157	InSb	0.1	CaF_2	Globar
1800–7000	8027	InSb	15	CaF_2	Tungsten
5000–9000	8027	Ge	87	CaF_2	Tungsten

surements of weak absorption bands. We have successfully applied it in the study of the high overtones of HDO,[13] D_2O,[14] and C_2H_2.[15] Some experimental details can also be found in Ref. 16. In the present study, it was applied to record the $\upsilon_{Si-H}=6$ overtone bands located around 12 345 cm^{-1} with a resolution of 0.25 cm^{-1} at the temperature about 296 K. An 81.9-cm-long sample cell was placed inside a 162-cm-long Ti:sapphire laser cavity. The sample cell was filled with 203 hPa of dichlorosilane. The interleaved rapid-scan method was applied, and the spectra were recorded at generation times (t_g) of 36, 56, and 76 μs. Same measurements but with empty sample cell were also carried out to get the base line. Figure 2 shows the spectra recorded at $t_g=56$ μs with (panel a) and without (panel b) sample gas. The transmittance spectrum of SiH_2Cl_2 (panel c) was obtained by a/b. We shall point out that it is essential to stabilize the laser emission in the measurements, otherwise it would be impossible to determine the integrated absorbance of this widely spread vibrational band.

Altogether 61 bands have been observed in the measurements, some of them can be readily assigned, others can also be assigned based on the *ab initio* calculation (see next section).

The vibrational band intensities can be derived from the integrated absorbance

$$I(\nu_0)=\int_{\nu_0-\nu_L}^{\nu_0+\nu_H}-\ln[S(\nu)/S_0(\nu)]d\nu/NL, \tag{2.1}$$

where ν_0 is the band center and ν_H and ν_L are the upper and lower limits which define the integral region of each band. The absorbance beside such region is believed to be negligible. $S(\nu)/S_0(\nu)$ defines the transmittance, L is the absorption path length, and N is the molecular density which can be deduced from the experimental conditions. The H_2O and HCl absorption lines were subtracted from the integration. To retrieve the intensity of the $\upsilon_{Si-H}=6$ band measured by FT-ICLAS, first the integrated absorbance at each generation time was obtained from direct integration, then a linear fit on the generation time (proportional to the equivalent absorption path length) was applied to get the band intensity. All the retrieved band intensities together with ν_L and ν_H are presented in Table II. Note that for those closely located bands, it is impossible to experimentally separate the band intensities from each other. In this case, the ν_L and ν_H were chosen to include all these overlapping bands and only the overall intensity value is given.

The uncertainties in the obtained experimental band intensity values may rise from (1) the uncertainty in base line determination which may introduce about 10% uncertainty and can be worse when the band is overlapped, (2) the un-

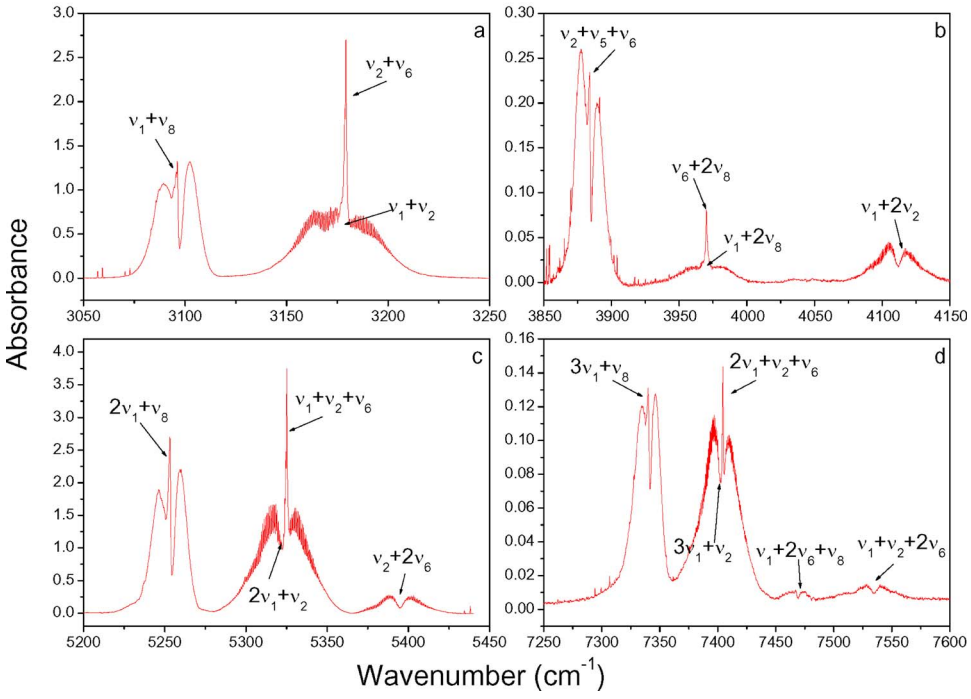

FIG. 1. (Color online) Some characteristic absorption bands of the SiH chromophore in SiH_2Cl_2. The experimental conditions are (a) sample pressure of 373 Pa and absorption path length of 15 m, (b) sample pressure of 8027 Pa and absorption path length of 15 m, and (c) and (d) sample pressure of 8027 Pa and absorption path length of 87 m.

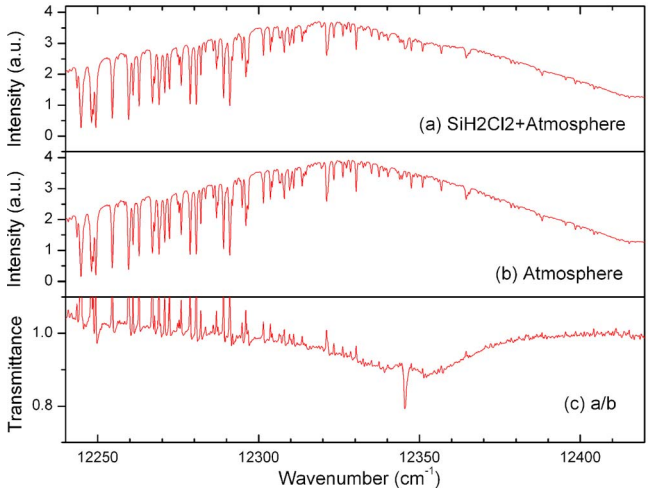

FIG. 2. (Color online) Absorption spectrum of the $\upsilon_{Si-H}=6$ band of SiH_2Cl_2 recorded by FT-ICLAS. The equivalent absorption path length is 4.5 km. Sample pressure: 203 hPa.

certainty in molecule density, which comes from the difficulty in the determination of the sample pressure (note that the SiH_2Cl_2 molecule can react with water vapor), the temperature fluctuation, and the absorption path length uncertainties, altogether about 5% for FTS measurements and about 10% for FT-ICLAS measurements, and (3) the limited signal-to-noise ratio (SNR) and nonlinear response of the instruments (for example, the detector). We estimate that the absolute intensity uncertainty is around 20% for moderate bands and may be worse for weak or overlapped ones.

III. FORCE FIELD CALCULATIONS AND VIBRATIONAL BANDS ASSIGNMENTS

SiH_2Cl_2 has nine vibration modes (see Table III). Upper states with symmetries of A_1, B_1, and B_2 can be accessed with *b*-, *c*-, and *a*-type transitions, respectively. While upper states with A_2 symmetry are infrared inactive. Because many

TABLE II. Observed band centers (in cm^{-1}) and intensities (in 10^{-22} cm) of SiH_2Cl_2. The symbol "↑" refers to band overlapped with adjacent ones. Band intensity is included in the value of the previous band.

Band	$\nu_{Obs.}$	$\nu_{Cal.-Obs.}$	ν_L/ν_H	$I_{Obs.}$	Band	$\nu_{Obs.}$	$\nu_{Cal.-Obs.}$	ν_L/ν_H	$I_{Obs.}$
ν_4	190[a]	0.0			$\nu_1+2\nu_2$	4 111.9	3.7	41.9/38.1	4.32
ν_3	527[a]	0.0			$2\nu_1$	4 389.1	1.5	49.1/40.9	399.6
ν_9	590[a]	0.0			$\nu_1+\nu_6$	4 392.2	0.7		↑
ν_7	602[a]	0.0			$2\nu_6$	4 463.3	0.5	23.3/26.7	79.18
ν_5	710[a]	0.1			$2\nu_1+\nu_7$	4 982.4	2.6	37.4/39.2	8.15
ν_8	876[a]	0.0			$\nu_1+\nu_6+\nu_7$	4 985.9	2.5		↑
ν_2	954[a]	0.0			$2\nu_6+\nu_7$	5 056.6	3.3	32.6/8.4	5.82
$\nu_4+\nu_8$	1066.8	2.3	26.8/18.2	505.6	$\nu_1+\nu_5+\nu_6$	5 091.3	5.0	26.3/27.7	29.15
$\nu_3+\nu_9$	1118.0	−3.9	33/25	1999	$2\nu_1+\nu_8$	5 253.1	1.4	39.1/23.9	39.07
$2\nu_7$	1204.8	−6.8	34.8/40.2	903.5	$2\nu_1+\nu_2$	5 323.0	3.2	46/42	53.23
$\nu_5+\nu_9$	1298.5	−2.3	7.5/31.5	320.2	$\nu_1+\nu_2+\nu_6$	5 325.1	3.1		↑
$\nu_5+\nu_7$	1319.9	3.7		↑	$\nu_2+2\nu_6$	5 394.9	4.4	29.9/35.9	7.14
$\nu_3+\nu_8$	1407.9	−7.4	37.9/67.1	1145	$2\nu_1+\nu_5+\nu_8$	5 951.0	3.2	1/2	0.0067
$2\nu_5$	1424.5	−0.2		↑	$\nu_1+\nu_2+\nu_5+\nu_6$	6 022.5	10.5	22.5/17.5	0.26
$\nu_2+\nu_7$	1553.0	−2.9	53/97	21.9	$3\nu_1$	6 483.9	2.6	45.9/41.1	10.85
$\nu_5+\nu_8$	1588.0	−3.8		↑	$2\nu_1+\nu_6$	6 483.9	2.7		↑
$2\nu_8$	1751.0	11.9	44/39	429.1	$\nu_1+2\nu_6$	6 610.8	0.5	38.8/44.2	5.76
$\nu_2+\nu_8$	1833.2	2.1	23.2/56.8	81.8	$3\nu_6$	6 634.5	4.3		↑
$2\nu_2$	1906.0	3.8	41/49	164.9	$3\nu_1+\nu_7$	7 070.8	6.7	50.8/39.2	1.44
ν_1	2224.0	0.0	49/61	71400	$2\nu_1+\nu_6+\nu_7$	7 072.8	5.1		↑
ν_6	2237.0	0.0		↑	$2\nu_1+\nu_5+\nu_6$	7 173.7	12.2	43.7/26.3	2.64
$\nu_2+\nu_5+\nu_8$	2543.7	1.1	33.7/46.3	16.1	$3\nu_1+\nu_8$	7 340.0	3.5	50/20	1.78
$\nu_1+\nu_7$	2823.5	−1.6	28.5/71.5	227.8	$3\nu_1+\nu_2$	7 403.5	8.5	43.5/41.5	1.98
$\nu_6+\nu_7$	2834.9	1.7		↑	$2\nu_1+\nu_2+\nu_6$	7 404.4	8.9		↑
$\nu_5+\nu_6$	2943.0	3.3	28/47	415.4	$\nu_1+2\nu_6+\nu_8$	7 467.2	3.8	18.2/16.8	0.054
$\nu_1+\nu_8$	3096.2	−1.4	26.2/23.8	1021	$\nu_1+\nu_2+2\nu_6$	7 534.6	4.1	24.6/25.4	0.086
$\nu_1+\nu_2$	3170.6	−1.8	40.6/59.4	1331	$4\nu_1$	8 506.0	5.5	56/44	3.45
$\nu_2+\nu_6$	3179.2	2.5		↑	$3\nu_1+\nu_6$	8 506.0	5.5		↑
$\nu_1+\nu_4+\nu_8$	3284.0	3.9	17/21	4.76	$\nu_1+3\nu_6$	8 714.6	6.5	14.6/15.4	0.017
$\nu_1+\nu_5+\nu_9$	3512.6	2.4	16/26	0.77	$6\nu_1$	12 345.4	12.8	50/40	0.0336
$\nu_1+2\nu_5$	3636.5	0.0	89/92	38.84	$5\nu_1+\nu_6$	12 345.4	12.8		↑
$\nu_1+\nu_2+\nu_7$	3764.2	−3.3	36.2/65.8	16.87	$7\nu_1$	14 161.8[b]	17.3		
$\nu_2+\nu_6+\nu_7$	3772.2	3.2		↑	$6\nu_1+\nu_6$	14 161.8[b]	17.3		
$\nu_1+\nu_5+\nu_8$	3800.8	−3.7		↑	$8\nu_1$	15 913.0[b]	18.8		
$\nu_2+\nu_5+\nu_6$	3883.9	8.2	37.9/29.1	18.43	$9\nu_1$	17 588.4[b]	27.9		
$\nu_1+2\nu_8$	3970.3	5.3	30.3/29.7	2.89					
$\nu_6+2\nu_8$	3970.3	13.1		↑					

[a]From Ref. 31.
[b]From Ref. 2.

TABLE III. Computed harmonic (ω_i) and fundamental (ν_i) frequencies (in cm^{-1}).

Symmetry	Mode	ω_i	ω_i (adjusted)	ν_i (adjusted)
$\nu_1(A_1)$	SiH_2 symmetric stretch	2334.4	2304.2	2224.0
$\nu_2(A_1)$	SiH_2 scissor	989.3	956.0	954.0
$\nu_3(A_1)$	$SiCl_2$ symmetric stretch	540.1	539.5	527.0
$\nu_4(A_1)$	$SiCl_2$ bend	190.1	184.7	190.0
$\nu_5(B_2)$	SiH_2 twist	732.8	704.4	710.1
$\nu_6(B_1)$	SiH_2 asymmetric stretch	2346.2	2314.2	2237.0
$\nu_7(B_1)$	SiH_2 rock	612.4	611.2	602.0
$\nu_8(B_2)$	SiH_2 wag	903.5	871.7	876.0
$\nu_9(B_2)$	$SiCl_2$ asymmetric stretch	605.0	595.2	590.0

vibrational bands are closely orientated, it is difficult to assign them correctly without any theoretical predictions. In this case, we carry out calculations based on the second-order perturbation theory with the calculated force constants of this molecule.

A. Force field calculation

We adopt the correlation consistent polarized valence basis sets (cc-pVnZ) of Dunning[17] and Woon and Dunning.[18] The cc-pVTZ basis set is used for H atom. Whereas for Si and Cl atoms it is replaced with cc-pVTZ+1 basis, which was derived from cc-pVTZ by adding a single set of d function whose exponent equals to the highest d exponent in the corresponding cc-pV5Z basis.[19] It is important to take into account core-polarization effects in the hard d function in the case of second-row atoms.[20] This mixed basis set was denoted as VTZ+1. This basis set was successfully applied in the anharmonic force field calculation on the $SiHCl_3$ molecule.[6] The geometry optimization and single point energies are calculated at the correlated level of MP2 method by using the GAUSSIAN03 program.[21] The obtained equilibrium structures are $R_{SiH}=1.4641$ Å, $R_{SiCl}=2.0414$ Å, $\phi_{HSiH}=112.523°$, and $\phi_{ClSiCl}=108.560°$. It agrees well with the experimental data.[22]

All force constants are determined based on the central difference formulas. Displacements have been set up in symmetrized internal coordinates and a step size of 0.01 Å or 0.5° was applied for stretching or bending motions, respectively. The symmetrized internal coordinates are defined as

$$S_1(A_1) = (r_1 + r_2)/\sqrt{2},$$

$$S_2(A_1) = (R_1 + R_2)/\sqrt{2},$$

$$S_3(A_1) = a\alpha - b(\theta_{11} + \theta_{12} + \theta_{21} + \theta_{22}),$$

$$S_4(A_1) = c\beta - d(\theta_{11} + \theta_{12} + \theta_{21} + \theta_{22}),$$

$$S_R(A_1) = e\alpha + f\beta + g(\theta_{11} + \theta_{12} + \theta_{21} + \theta_{22}),$$

$$S_5(A_2) = (-\theta_{11} + \theta_{12} + \theta_{21} - \theta_{22})/2, \tag{3.1}$$

$$S_6(B_1) = (r_1 - r_2)/\sqrt{2},$$

$$S_7(B_1) = (-\theta_{11} - \theta_{12} + \theta_{21} + \theta_{22})/2,$$

$$S_8(B_2) = (R_1 - R_2)/\sqrt{2},$$

$$S_9(B_2) = (-\theta_{11} + \theta_{12} - \theta_{21} + \theta_{22})/2,$$

$$a = 0.893\,45, \quad b = 0.224\,58,$$

$$c = 0.901\,48, \quad d = 0.216\,41,$$

$$e = 2\sin(\alpha/2)\cos(\beta/2)/N = 0.412\,78,$$

$$f = 2\cos(\alpha/2)\sin(\beta/2)/N = 0.394\,22,$$

$$g = \sin\theta/N = 0.410\,55,$$

where r_i and R_j are the displacement of the SiH_i and $SiCl_j$ bond lengths, respectively. α, β, and θ_{ij} are the displacements of H–Si–H, Cl–Si–Cl, and H_i–Si–Cl_j angles, respectively. a, b, c, and d are determined from the orthonormality conditions. The potential-energy expansion in the symmetrized internal coordinates is given as

$$V = V_0 + \frac{1}{2}\sum_{i,j} F_{ij}S_iS_j + \frac{1}{6}\sum_{i,j,k} F_{ijk}S_iS_jS_k + \frac{1}{24}\sum_{i,j,k,l} F_{ijkl}S_iS_jS_kS_l. \tag{3.2}$$

There are, altogether, 18 quadratic, 52 cubic, and 147 quartic force constants, which are listed in Table IV. All the force constants in symmetrized internal coordinates are transformed to those in normal coordinates through the L tensor.[23] Spectroscopic constants are obtained based on the second-order perturbation theory by using the SPECTRO program.[24]

B. Vibrational bands assignments

All the harmonic and fundamental frequencies of SiH_2Cl_2 are given in Table III. No vibrational interaction has been included at current stage. The anharmonic correction $\omega_i - \nu_i$ values are derived from the anharmonic constants x_{ij} which have been calculated under standard formulas from perturbation theory.[25] We have iteratively adjusted the nine diagonal quadratic force constants so that the nine calculated fundamental frequencies of SiH_2Cl_2 can exactly reproduce the experimental values. The final adjusted quadratic force constants are given in the caption of Table IV. Based on the second-order perturbation formulas for asymmetric top molecules, the anharmonic constants x_{rs}, k_{rrss} are also obtained, which are presented in Table V together with other spectroscopic constants.

The anharmonic constants x_{11}, x_{66}, and k_{1166} exactly fulfill the empirical x, K relations[26] between the symmetric and asymmetric stretching vibrations of SiH_2, which are

TABLE IV. Quadratic, cubic, and quartic force constants. Energy in units of aJ and coordinates in units of Å or rad. The adjusted force constants are F_{11} =3.089 59, F_{22}=3.351 27, F_{33}=0.516 18, F_{44}=0.725 00, F_{55}=0.416 20, F_{66}=3.031 04, F_{77}=0.741 23, F_{88}=2.918 53, and F_{99}=0.608 53.

i	j	k	F_{ij}/F_{ijk}	i	j	k	l	F_{ijk}/F_{ijkl}	i	j	k	l	F_{ijkl}	i	j	k	l	F_{ijkl}	i	j	k	l	F_{ijkl}	i	j	k	l	F_{ijkl}
1	1		3.171 04	6	6	2		0.077 60	4	4	4	4	13.231 00	4	4	8	8	−0.752 08	3	3	7	7	0.827 46	9	9	1	3	−0.065 63
2	2		3.348 63	7	7	2		−0.583 37	5	5	5	5	1.804 65	5	5	8	8	0.300 83	4	4	6	6	0.150 76	5	5	1	4	−0.032 82
3	3		0.546 94	8	8	2		−9.857 83	9	9	9	9	7.066 49	6	6	9	9	0.000 00	9	9	2	3	−1.016 92	5	5	6	7	−0.000 08
4	4		0.762 06	9	9	2		−0.616 57	2	2	2	1	0.283 39	1	1	2	3	0.037 46	9	9	9	8	−0.393 57	6	6	1	4	0.024 99
5	5		0.450 47	6	7	2		0.157 37	3	3	3	2	−0.475 68	1	1	8	9	0.087 47	1	3	6	7	−0.085 87	6	6	6	7	0.037 43
6	6		3.115 55	8	9	2		0.284 27	4	4	4	3	−8.175 25	2	2	6	7	−0.249 82	2	3	6	7	−0.003 58	7	7	1	4	−0.049 11
7	7		0.744 17	5	6	9		−0.075 14	1	1	5	5	−0.087 04	3	3	2	4	1.131 70	3	4	6	7	−0.012 31	7	7	7	6	0.016 37
8	8		3.010 53	3	3	3		−0.053 79	1	1	9	9	−0.174 27	4	4	1	3	−0.000 04	1	5	6	9	−0.100 20	8	8	1	4	−0.049 92
9	9		0.651 52	1	1	4		−0.009 24	2	2	6	6	0.087 43	4	5	6	9	−0.008 22	4	4	1	2	−0.042 92	8	8	6	7	−0.149 94
1	2		0.097 07	3	3	1		−0.209 82	3	3	4	4	6.991 45	4	4	9	9	7.066 49	4	4	8	9	−0.131 11	9	9	1	4	0.000 00
1	3		0.058 81	4	4	2		−0.977 81	3	3	8	8	0.000 34	5	5	9	9	−0.150 42	5	5	2	3	−0.032 82	9	9	2	4	1.508 93
1	4		−0.022 61	1	3	4		0.028 55	4	4	7	7	1.654 07	7	7	8	8	0.150 42	5	5	8	9	−0.327 86	1	2	3	4	0.082 28
2	3		−0.170 13	5	5	3		0.002 63	5	5	7	7	0.902 50	1	1	2	4	0.012 52	6	6	2	3	−0.037 46	1	3	8	9	0.075 14
2	4		0.145 39	6	6	3		0.106 16	6	6	8	8	0.000 00	2	2	1	3	−0.087 44	6	6	8	9	0.049 98	2	4	6	7	0.143 12
3	4		−0.250 28	7	7	3		−0.069 21	8	8	9	9	0.087 23	2	2	8	9	−0.224 80	7	7	2	3	−0.065 67	3	4	8	9	−0.024 59
6	7		−0.037 70	8	8	3		0.070 94	1	1	6	7	0.037 46	3	3	6	7	−0.016 45	7	7	8	9	−0.426 31	1	5	7	8	0.178 92
8	9		−0.298 02	9	9	3		0.848 24	2	2	3	4	−0.758 56	4	4	2	4	34.617 96	8	8	2	3	−0.049 98	9	9	3	4	−4.247 38
1	1	1	−9.865 02	6	7	3		−0.017 82	6	6	6	6	28.730 81	4	5	7	8	−0.139 34	8	8	8	9	−0.199 76	1	2	6	7	0.074 936
1	1	2	−0.010 68	2	3	4		0.273 79	1	1	1	2	−0.207 08	5	5	6	6	0.601 67	4	4	5	5	0.000 00	1	4	6	7	−0.025 03
2	2	3	0.221 32	5	5	4		0.400 17	2	2	2	3	−0.224 86	6	6	7	7	0.348 94	5	5	1	2	0.171 76	2	3	8	9	0.168 18
3	3	4	−0.706 54	6	6	4		−0.055 45	3	3	3	4	−3.401 67	7	7	9	9	0.300 83	5	5	2	4	−0.393 60	6	7	8	9	0.164 58
1	2	3	0.043 03	7	7	4		−0.008 20	1	1	2	2	0.043 815	1	1	3	4	−0.028 67	6	6	1	2	−0.130 85	1	5	7	9	−0.024 61
5	5	1	−0.091 60	8	8	4		0.193 34	1	1	6	6	27.815 46	2	2	1	4	−0.162 35	6	6	2	4	0.025 10	9	9	6	7	0.016 33
6	6	1	−9.716 57	9	9	4		−1.147 38	2	2	3	3	0.305 318	3	3	1	2	−0.04292	7	7	1	2	0.128 77	1	2	8	9	−0.156 14
7	7	1	−0.086 16	6	7	4		−0.034 64	2	2	7	7	0.610 54	3	3	8	9	−0.065 56	7	7	2	4	0.377 27	1	4	8	9	0.042 92
8	8	1	−0.169 59	8	9	4		−0.080 15	3	3	5	5	−0.150 07	4	4	6	7	0.032 78	8	8	1	2	0.283 36	2	4	8	9	0.035 80
9	9	1	−0.058 39	5	7	9		0.422 64	3	3	9	9	2.556 39	4	5	7	9	0.131 55	8	8	2	4	−0.299 66	1	5	6	8	0.043 73
6	7	1	−0.040 28	8	9	3		−0.161 01	7	7	7	7	2.030 11	3	3	1	4	−0.032 78	9	9	1	2	0.057 27	2	5	6	8	−0.237 30
8	9	1	0.121 40	5	7	8		−0.374 41	1	1	1	3	−0.024 96	8	8	8	8	27.815 26	5	5	1	3	0.000 00	2	5	6	9	0.157 44
5	6	8	0.117 28	4	4	4		−2.420 40	2	2	2	4	1.249 00	1	1	1	4	0.062 48	5	5	3	4	0.300 75	3	5	6	9	0.008 20
2	2	2	−10.371 84	2	2	1		−0.260 93	4	4	4	1	−0.049 19	3	3	3	1	0.180 41	6	6	1	3	−0.124 90	2	5	7	8	0.264 76
1	1	3	−0.075 69	3	3	2		−0.184 34	1	1	3	3	0.043 815	4	4	4	2	4.001 80	6	6	3	4	−0.028 64	3	5	7	8	−0.123 00
2	2	4	−0.483 10	4	4	3		1.595 45	1	1	7	7	−0.086 94	1	1	4	4	0.000 20	7	7	1	3	0.016 45	2	5	7	9	−0.410 03
4	4	1	−0.014 60	1	1	1	1	27.815 46	2	2	4	4	1.613 13	1	1	8	8	−0.087 23	7	7	3	4	−0.169 18	3	5	7	9	−0.004 69
1	2	4	0.050 15	2	2	2	2	28.600 16	2	2	8	8	27.815 06	2	2	5	5	0.087 23	8	8	1	3	−0.049 98	3	5	6	8	0.025 07
5	5	2	−0.251 04	3	3	3	3	2.556 39	3	3	6	6	0.000 34	2	2	9	9	0.697 67	8	8	3	4	0.200 33	4	5	6	8	0.071 528

$$x_{11} \doteq x_{66} \doteq \frac{x_{16}}{4} \doteq \frac{k_{1166}}{4} = \frac{x_m}{2},$$

$$\omega_m = \frac{\omega_1 + \omega_2}{2}, \tag{3.3}$$

$$\lambda = \frac{\omega_1 - \omega_2}{2}.$$

Here ω_m, x_m, and λ are, respectively, the harmonic, anharmonic, and coupling constants in the local-mode interpretation of the SiH_2 stretching vibrations. According to the relations, x_m is about $-34\ \mathrm{cm}^{-1}$, which agrees well with the corresponding value of silane.[27] Here we adopt a simplified effective Hamiltonian by neglecting all the resonance interactions except the Darling-Dennison resonance between the ν_1 and ν_6 modes. The diagonal elements of the Hamiltonian matrix are in the form

$$\tilde{H}_{VV} = \left(\sum_{i=1}^{9} \tilde{\omega}_i \left(\nu_i + \frac{1}{2} \right) + \sum_{i=1}^{9} \sum_{j=i}^{9} \tilde{x}_{ij} \left(\nu_i + \frac{1}{2} \right) \left(\nu_j + \frac{1}{2} \right) \right) \times |\nu_1, \ldots, \nu_9\rangle\langle \nu_1, \ldots, \nu_9|, \tag{3.4}$$

and the nonvanishing off-diagonal elements are like

$$\tilde{H}_{VV'} = \frac{k_{1166}}{4} [(\nu_6 + 1)(\nu_6 + 2)\nu_1(\nu_1 - 1)/2]^{1/2} |\nu_1, \ldots, \nu_6, \ldots, \nu_9\rangle\langle \nu_1 - 2, \ldots, \nu_6 + 2, \ldots, \nu_9|. \tag{3.5}$$

The energy values of the upper states can be obtained by explicit diagonalization of the effective Hamiltonian matrix. Based on these calculated results, observed band intensities, and symmetry, 61 bands are assigned. The assignments, observed band centers, and the differences between calculated and observed values are given in Table II. It seems to be reasonable to use the simplified Hamiltonian model since the

TABLE V. Calculated anharmonic and spectroscopic constants (in cm^{-1}) of SiH_2Cl_2 and some available experimental values.

r	s	x_{rs}	k_{rrss}	r	s	x_{rs}	k_{rrss}	P	Calc.	Obs.[a]	P	Calc.
1	1	−17.110		2	9	1.124	−91.122	A_0	0.472 094	0.471 5(27)	$\alpha_9^A\times10^3$	3.716 58
2	2	0.964		3	4	−8.289	−8.202	B_0	0.084 833	0.085 8(7)		
3	3	−1.638		3	5	1.106	1.160	C_0	0.073 792	0.074 5(7)	$\alpha_1^B\times10^3$	0.015 30
4	4	0.869		3	6	0.153	0.102	$D_J\times10^7$	0.339 35	0.334 23	$\alpha_2^B\times10^3$	0.652 08
5	5	2.029		3	7	−2.404	−0.513	$D_{JK}\times10^5$	0.495 60	0.473 99	$\alpha_3^B\times10^3$	0.399 54
6	6	−16.700		3	8	−2.508	0.280	$D_K\times10^6$	−0.540 33	−0.515 69	$\alpha_4^B\times10^3$	0.036 04
7	7	−2.984		3	9	−2.912	4.672	$d_J\times10^8$	0.808 04	0.804 07	$\alpha_5^B\times10^3$	−0.646 21
8	8	4.974		4	5	2.029	−66.238	$d_K\times10^7$	0.963 52	1.039 7	$\alpha_6^B\times10^3$	−0.013 58
9	9	−1.657		4	6	−0.44	−6.612	$H_J\times10^{13}$	0.297 53		$\alpha_7^B\times10^3$	0.407 12
1	2	−9.104	−35.292	4	7	−0.262	−0.061	$H_{JK}\times10^{14}$	−0.343 70		$\alpha_8^B\times10^3$	0.744 97
1	3	−0.111	−2.404	4	8	3.162	7.309	$H_{KJ}\times10^{10}$	−0.220 92		$\alpha_9^B\times10^3$	0.265 47
1	4	−0.083	−0.116	4	9	−0.977	−2.893	$H_K\times10^9$	0.192 17			
1	5	−5.859	−50.999	5	6	−0.806	−201.844	$h_1\times10^{13}$	0.144 97		$\alpha_1^C\times10^3$	0.000 61
1	6	−68.081	−68.839	5	7	11.480	−3.763	$h_2\times10^{14}$	0.168 14		$\alpha_2^C\times10^3$	0.176 56
1	7	−4.055	−56.053	5	8	−1.890	−7.910				$\alpha_3^C\times10^3$	0.387 13
1	8	−5.171	−42.808	5	9	−3.831	−0.933	$\alpha_1^A\times10^3$	0.482 45		$\alpha_4^C\times10^3$	0.096 52
1	9	0.579	−6.782	6	7	−2.404	−158.212	$\alpha_2^A\times10^3$	−5.814 95		$\alpha_5^C\times10^3$	−0.459 39
2	3	−3.498	−2.772	6	8	−7.747	−309.462	$\alpha_3^A\times10^3$	−0.852 18		$\alpha_6^C\times10^3$	−0.014 39
2	4	11.933	−0.404	6	9	1.048	−1.115	$\alpha_4^A\times10^3$	−4.380 31		$\alpha_7^C\times10^3$	0.466 39
2	5	1.102	−14.891	7	8	−3.452	−8.327	$\alpha_5^A\times10^3$	7.583 39		$\alpha_8^C\times10^3$	0.609 05
2	6	−9.247	−126.79	7	9	0.456	−1.564	$\alpha_6^A\times10^3$	0.321 00		$\alpha_9^C\times10^3$	0.025 86
2	7	−5.859	−0.612	8	9	0.665	−0.681	$\alpha_7^A\times10^3$	−5.934 42			
2	8	5.617	1.590					$\alpha_8^A\times10^3$	−6.674 80			

[a]From Ref. 22.

largest deviation is 27.9 cm^{-1} which comes from the eighth overtone.

IV. REDUCED-DIMENSIONAL DIPOLE MOMENT SURFACE AND BAND INTENSITIES

Because most of the observed overtones are due to the SiH_2 vibrations (Si–H stretching and H–Si–H bending) and these vibration modes are well separated from other modes in this molecule, here we just concentrate on the SiH_2 vibrational bands and the related dipole moments. In order to get this *ab initio* reduced-dimensional dipole moment surface, the $SiCl_2$ part is kept on its equilibrium configurations, and an oriented bisector frame (see Fig. 3) is used. The origin of the coordinates system coincides with the silicon atom, z axis bisects the H–Si–H and Cl–Si–Cl angles, x axis is in the SiH_2 plane, and y axis is in the $SiCl_2$ plane. The dipole moment is obtained from the energy derivatives with respect to an external electric field. A finite field of $\pm0.005E_h/ea_0$ along the bisector axis is adopted. All single point energies are calculated at the MP2 level with cc-PVTZ+1 basis sets.

The dipole moment vectors are projected to the bisector frame as

$$\mathbf{M}(r_1,r_2,r_3)=u_x(r_1,r_2,\theta)\mathbf{e}_x+u_z(r_1,r_2,\theta)\mathbf{e}_z. \tag{4.1}$$

The dipole moment x and z components can be expanded with a polynomial function of the displacements on the internal coordinates Δr_1, Δr_2, and $\Delta\theta$.

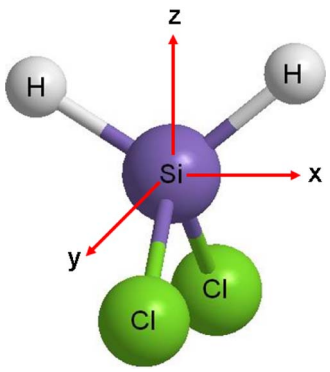

FIG. 3. (Color online) Bisector frame and definition of the x, y, and z coordinate systems used in *ab initio* calculations. The z axis bisects the H–Si–H and Cl–Si–Cl bond angles.

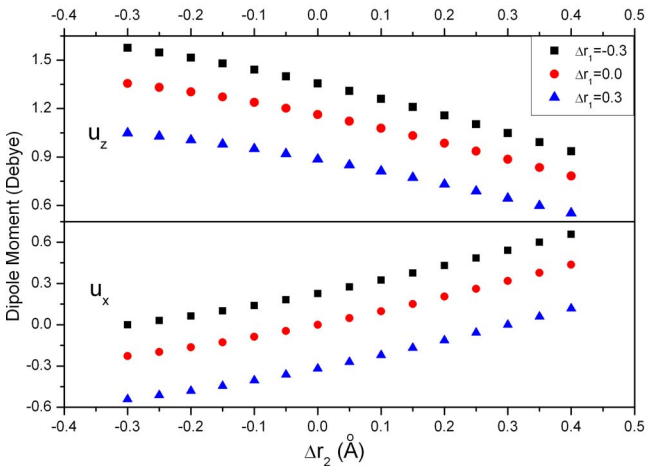

FIG. 4. (Color online) Dipole moments u_z and u_x at different displacements of the Si–H bond lengths.

TABLE VI. *Ab initio* calculated values of the SiH_2Cl_2 dipole moment expansion coefficients (in Debye).

z component	3D	2D	x component	3D	2D
D^z_{000}	0.581 438(12)	0.581 416(02)	D^x_{100}	−0.932 612(38)	−0.932 209(46)
D^z_{100}	−0.805 528(76)	−0.805 880(17)	D^x_{200}	−0.511 97(21)	−0.513 06(25)
D^z_{200}	−0.485 29(45)	−0.473 737(97)	D^x_{300}	0.254 27(46)	0.253 06(62)
D^z_{300}	0.252 60(91)	0.255 95(22)	D^x_{210}	−0.078 99(35)	−0.075 66(45)
D^z_{400}	0.070 9(36)	0.063 50(80)	D^x_{400}	0.074 1(18)	0.080 9(22)
D^z_{310}	−0.139 1(30)	−0.124 42(66)	D^x_{310}	0.022 0(16)	0.040 1(19)
D^z_{220}	0.037 3(21)	0.026 39(47)	D^x_{101}	0.541 24(19)	
D^z_{110}	0.184 15(26)	0.182 738(56)	D^x_{201}	0.109 57(33)	
D^z_{210}	0.065 68(75)	0.067 26(18)	D^x_{301}	−0.157 9(15)	
D^z_{001}	0.766 900(49)		D^x_{211}	0.269 8(13)	
D^z_{101}	0.015 71(37)		D^x_{102}	0.062 72(28)	
D^z_{201}	0.278 29(65)		D^x_{202}	0.104 4(14)	
D^z_{301}	0.036 3(30)		D^x_{103}	−0.037 7(14)	
D^z_{111}	−0.291 24(40)				
D^z_{211}	−0.126 0(25)				
D^z_{002}	0.050 33(33)				
D^z_{102}	−0.079 39(57)				
D^z_{202}	−0.107 2(28)				
D^z_{112}	0.187 0(18)				
D^z_{003}	−0.119 50(43)				
D^z_{103}	−0.048 5(28)				
D^z_{004}	0.018 1(23)				
rms($\times 10^{-4}$)	2.21	0.18		1.05	0.47

$$\mu^{\alpha}(\Delta r_1, \Delta r_2, \Delta\theta) = \sum_{i,j,k} D^{\alpha}_{ijk} \Delta r_1^i \Delta r_2^j \Delta\alpha^k. \tag{4.2}$$

Here the coefficients follow the simple relations $D^x_{ijk} = -D^x_{jik}$ and $D^z_{ijk} = D^z_{jik}$, which are similar to those of H_2S molecule.[28]

Ab initio dipole moment calculations are carried out for two sets of geometrical configurations. At the first step (set I, 2D), 120 geometries are calculated with the bond length displacements ranging from −0.3 to 0.4 Å with a step of 0.05 Å. At the second step (set II, 3D), we calculate 1020 geometries not only with the bond length displacements like set I but also with the H–Si–H angle displacements ranging from −20° to 20° with a step of 5°. In Fig. 4, the dipole moments along the x and z axes are presented at different displacements of the Si–H bond lengths. The analytical dipole moment functions are then derived by fitting these calculated values according to Eq. (4.2). The resulted dipole moment coefficients are listed in Table VI.

The absolute band intensities can be calculated as

$$I = K\nu |\langle N|M|0\rangle|^2, \tag{4.3}$$

where K is a constant coefficient, ν is the band center, and $|N\rangle$ and $|0\rangle$ denote the eigenvectors of the excited and ground states, respectively. M is the reduced-dimensional dipole moment surface discussed above. The vibrational wave functions are calculated variationally based on the simple curvilinear internal coordinate Hamiltonian which has been proposed by Halonen.[29] More details about the Hamiltonian

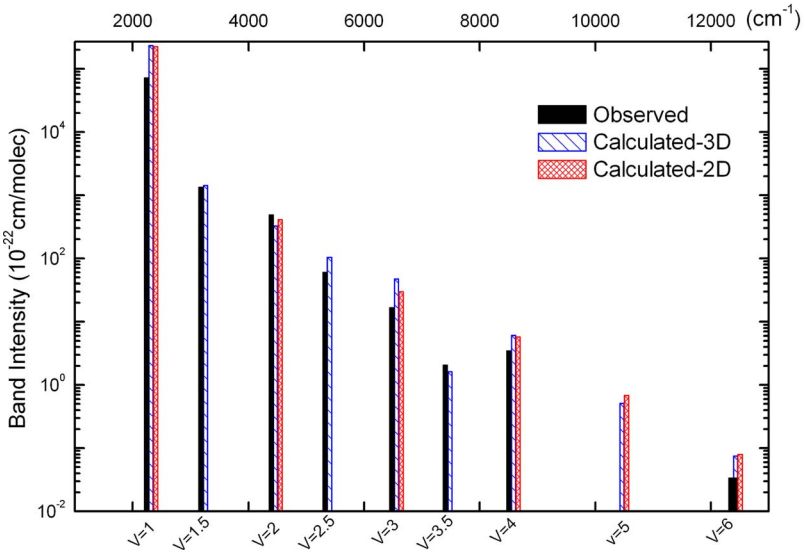

FIG. 5. (Color online) Total band intensities of different polyad $[V = \upsilon_1 + \upsilon_6 + (1/2)\upsilon_2]$: observed and calculated (with 3D or 2D dipole moment functions) values.

TABLE VII. Kinetic- and potential-energy parameters of dichlorosilane. Uncertainties in parentheses are one standard deviations in the last digit.

$g^0_{rr}(u^{-1})$	1.027 979	$D_e(aJ)$	0.760 97(84)
$g^0_{\theta\theta}(u^{-1}\ \text{Å}^{-2})$	0.967 885	$\alpha(\text{Å}^{-1})$	1.414 80(86)
$g^0_{rr'}(u^{-1})$	−0.013 650	$f_{\theta\theta}(aJ)$	0.576 55(84)
$g^0_{r\theta}(u^{-1}\ \text{Å}^{-1})$	−0.022 517	$f_{rr'}(aJ\ \text{Å}^{-2})$	0.021 880(84)
$\left(\frac{\partial g_{\theta\theta}}{\partial r}\right)_e(u^{-1}\ \text{Å}^{-3})$	−0.659 727	$f^b_{r\theta}(aJ\ \text{Å}^{-1})$	0.0[a]
$\left(\frac{\partial g_{r\theta}}{\partial \theta}\right)_e(u^{-1}\ \text{Å}^{-1})$	0.009 304	$f_{r\theta\theta}(aJ\ \text{Å}^{-1})$	−0.265(10)

[a]Constrained values.

can be found in Ref. 29 and here we just give a brief description. The Hamiltonian only includes the Si–H stretching and H–Si–H bending modes. It takes the form

$$H = H_0 + H_1, \tag{4.4}$$

where

$$\begin{aligned} H_0 = {} & \frac{1}{2}g^0_{rr}(p_1^2+p_2^2) + \frac{1}{2}g^0_{\theta\theta}p_\theta^2 + g^0_{rr'}p_1p_2 + g^0_{r\theta}(p_1+p_2)p_\theta \\ & + D_e(y_1^2+y_2^2) + \frac{1}{2}f_{\theta\theta}\theta^2 + \alpha^{-2}f_{rr'}y_1y_2 + \alpha^{-1}f_{r\theta}(y_1 \\ & + y_2)\theta, \\ H_1 = {} & \frac{1}{2}\alpha^{-1}\left(\frac{\partial g_{\theta\theta}}{\partial r}\right)_e(y_1+y_2)p_\theta^2 + \frac{1}{2}\left(\frac{\partial g_{r\theta}}{\partial \theta}\right)_e(p_1+p_2)(p_\theta\theta \\ & + \theta p_\theta) + \frac{1}{2}\alpha^{-1}f_{r\theta\theta}(y_1+y_2)\theta^2. \end{aligned} \tag{4.5}$$

p_1, p_2, and p_θ are momentum operators conjugate to the curvilinear internal coordinates r_1, r_2, and θ. The G matrix elements and their derivatives evaluated at the equilibrium configurations are obtained from the book of Wilson *et al.*[30] The explicit expression of the coefficients can be found in Ref. 29 and θ=112.45° is used here. D_e and α are the Morse parameters. The six potential-energy parameters are optimized by the nonlinear least-squares method using 29 vibrational band centers related to SiH_2. The basis-set size is restricted by $m+n\leqslant 9$ and $\nu\leqslant 4$, where m and n are quantum numbers for the Si–H stretching motions and ν for the scissoring SiH_2 bending motion. The Morse basis functions for the stretching states are chosen to be consistent with the Morse parameters D_e and α. The harmonic oscillator basis functions for the scissoring vibration are chosen to be consistent with the harmonic force constant $f_{\theta\theta}$. The G matrix elements and the fitted potential-energy parameters are given in Table VII. The standard deviation of the fit is 1.2 cm^{-1}. Put in the wave functions and the dipole moment function (2D or 3D) into Eq. (4.3), we can get the vibrational band intensities. The calculated values are presented in Table VIII. It can be found that most of the calculated band intensities are within 0.6–3.0 times of the experimental values. As an illustration, the observed and calculated (2D and 3D, respectively) total band intensities of different polyads $[V=v_1+v_6+(1/2)v_2]$ are presented in Fig. 5.

From Fig. 5, as well as Table VIII, we can find that for most vibrational polyads, the calculated intensities (both 2D and 3D results) agree reasonably with the observed values. The largest discrepancy takes place at the fundamental bands $V=1$. The calculated value is about three times of the observed one. First question may be raised that if this discrepancy comes from improper neglect of the $SiCl_2$ motion in the dimethyl sulfide (DMS) model. Since the $SiCl_2$ group has been fixed at the equilibrium structure to simplify our DMS model, the effects from the SiH_2 wag, rock, and twist modes have been neglected. As a comparison, we perform full-dimensional *ab initio* anharmonic frequency calculation at MP2 level with cc-PVTZ basis sets. The differences in the optimized structure compared with the equilibrium structure obtained from the cc-PVTZ+1 basis sets are within 0.007 Å for bond lengths and within 1.4° for angles. In this case, the calculated band intensities are 9.04×10^4 and 6.30×10^4 (in 10^{-22} cm^{-1}/molecule) for ν_1 and ν_6, respectively. The total value is still more than two times of the observed one. It

TABLE VIII. Observed and calculated band intensities (in 10^{-22} cm/molecule). This symbol "↑" refers to band overlapped with adjacent ones. Band intensity is included in the value of the previous band.

Band	$\nu_{\text{Calc.}}$ (in cm^{-1})	$I_{\text{Obs.}}$	$I_{\text{Calc.}}$[a]	$I_{\text{Calc.}}$[b]	Band	$\nu_{\text{Calc.}}$ (in cm^{-1})	$I_{\text{Obs.}}$	$I_{\text{Calc.}}$[a]	$I_{\text{Calc.}}$[b]
$2\nu_2$	1907.38	1.64*E*+2	2.79*E*+2	⋯	$3\nu_1$	6 482.89	1.09*E*+1	9.43*E*+0	1.43*E*+1
ν_6	2236.26	7.14*E*+4	1.31*E*+5	1.31*E*+5	$2\nu_1+\nu_6$	6 483.00	↑	1.21*E*+1	1.15*E*+1
ν_1	2224.65	↑	1.04*E*+5	9.40*E*+4	$\nu_1+2\nu_6$	6 612.80	5.76*E*+0	2.39*E*+1	3.39*E*+0
$\nu_2+\nu_6$	3179.34	1.33*E*+3	9.67*E*+2	⋯	$3\nu_6$	6 635.11	↑	1.71*E*+0	5.40*E*−1
$\nu_1+\nu_2$	3169.67	↑	4.61*E*+2	⋯	$2\nu_1+\nu_2+\nu_6$	7 404.16	1.98*E*+0	1.13*E*+0	⋯
$\nu_1+2\nu_2$	4110.16	5.06*E*+0	7.18*E*+0	⋯	$3\nu_1+\nu_2$	7 403.87	↑	4.17*E*−2	⋯
$\nu_1+\nu_6$	4391.94	4.00*E*+2	1.66*E*+2	1.95*E*+2	$\nu_1+\nu_2+2\nu_6$	7 534.56	8.58*E*−2	4.34*E*−1	⋯
$2\nu_1$	4389.62	↑	1.30*E*+2	1.19*E*+2	$4\nu_1$	8 505.75	3.45*E*+0	3.37*E*+0	3.22*E*+0
$2\nu_6$	4463.28	7.92*E*+1	1.85*E*+1	1.17*E*+2	$3\nu_1+\nu_6$	8 505.81	↑	2.70*E*+0	2.37*E*+0
$2\nu_1+\nu_2$	5322.81	5.32*E*+1	5.31*E*+1	⋯	$\nu_1+3\nu_6$	8 717.07	1.7*E*−2	6.45*E*−4	4.64*E*−2
$\nu_1+\nu_2+\nu_6$	5324.00	↑	4.23*E*+1	⋯	$6\nu_1$	12 344.48	3.36*E*−2	7.51*E*−2	4.54*E*−2
$\nu_2+2\nu_6$	5394.90	7.14*E*+0	7.91*E*+0	⋯	$5\nu_1+\nu_6$	12 344.54	↑	9.33*E*−3	5.32*E*−3

[a]Calculated with 3D DMS.
[b]Calculated with 2D DMS. See text for details.

indicates that the dimension reduction is acceptable under present precision of the *ab initio* calculation.

We also carry out the analysis on the contributions from different terms to the transition dipole moments. We can find that for all the bands calculated with 2D DMS and most bands calculated with 3D DMS, the band intensity mainly comes from the direct transition from the zeroth-order local-mode ground-state wave function to the corresponding zeroth-order upper-state wave function. It means that the mixing of the wave functions due to resonance interactions does not give any significant contribution to the band intensities. For $2\nu_6$ and $\nu_1+3\nu_6$ bands, the 3D model underestimates the band intensities by 4 and 25 times, respectively. The reason is that the contribution from the bending part in the dipole moment function cancels the one from other parts, thus higher-order terms which cannot be well calculated in the dipole moment model plays a much more important role in the transition moment. It also implies that the band intensity is very sensitive to the DMS model.

It is also worthy to note those bands with one or several ν_8 (SiH_2 wag mode) quanta excited. The intensities of these bands are quite close to corresponding bands if ν_2 is replaced by ν_8. Note that the frequency of ν_8 mode is close to ν_2. So possibly the $\nu_2-\nu_8$ interaction plays a role in the molecule.

V. CONCLUSION

In this work, the vibrational overtones of SiH_2Cl_2 have been studied with Fourier-transform spectroscopy and sensitive Fourier-transform intracavity laser absorption spectroscopy. Experimental band intensities are also derived from the spectra. An anharmonic quartic force field is obtained by using the MP2 theory and cc-pVTZ+1 basis set under the frozen-core approximation. From the *ab initio* calculated and a minor empirical adjusted force field, fundamental frequencies are derived based on second-order perturbation theory. Based on the predictions given by the vibrational study with an effective Hamiltonian, 59 new bands are assigned and the predictions agree well with the observed values. The rovibrational spectroscopic constants were also presented which give satisfied agreements with available experimental results. Reduced-dimensional *ab initio* dipole moment surfaces of the isolated SiH_2 chromophore (including Si–H stretching and H–Si–H bending) are calculated and applied to derive an analytical presentation in terms of the internal coordinate. A simple curvilinear coordinate Hamiltonian is employed to calculate the absolute band intensity. The calculated intensities agree well with most of the experimental data. The discrepancies between the calculated and observed values are also discussed.

ACKNOWLEDGMENTS

This work was jointly supported by the National Natural Science Foundation of China (20103007 and 20473079) and the National Project for the Development of Key Fundamental Sciences in China.

[1] H. Bürger and A. Ruoff, Spectrochim. Acta, Part A **26**, 1449 (1970).
[2] R. A. Bernheim, F. W. Lampe, J. F. O'Keefe, and J. R. Qualey III, Chem. Phys. Lett. **100**, 45 (1983).
[3] A. Campargue, F. Stoeckel, and M. C. Terrile, Chem. Phys. **110**, 145 (1986).
[4] Y. Ding, S.-G. He, J.-J. Zheng, S.-M. Hu, X.-H. Wang, and Q.-S. Zhu, Mol. Phys. **99**, 1669 (2001).
[5] S.-G. He, H. Lin, H. Bürger, W. Thiel, Y. Ding, and Q.-S. Zhu, J. Chem. Phys. **116**, 105 (2002).
[6] J.-J. Zheng, S.-G. He, S.-M. Hu, and Q.-S. Zhu, Mol. Phys. **101**, 1165 (2003).
[7] R. W. Davis and M. C. L. Gerry, J. Mol. Spectrosc. **60**, 117 (1976).
[8] J. A. Hawkins and M. K. Wilson, J. Chem. Phys. **21**, 360 (1953).
[9] R. W. Davis, A. G. Robiette, and M. C. L. Gerry, J. Mol. Spectrosc. **85**, 399 (1981).
[10] C. Møller and M. S. Plesset, Phys. Rev. **46**, 618 (1934).
[11] J. Demaison, L. Margulès, J. Breidung, W. Thiel, and H. Bürger, Mol. Phys. **97**, 1053 (1999).
[12] J. F. D'Eu, J. Demaison, and H. Bürger, J. Mol. Spectrosc. **218**, 12 (2003).
[13] S.-M. Hu, H. Lin, S.-G. He, J.-X. Cheng, and Q.-S. Zhu, Phys. Chem. Chem. Phys. **1**, 3727 (1999).
[14] S.-M. Hu, O. N. Ulenikov, E. S. Bekhtereva, G. A. Onopenko, S.-G. He, H. Lin, J.-X. Cheng, and Q.-S. Zhu, J. Mol. Spectrosc. **212**, 89 (2002).
[15] S.-M. Hu, A. Campargue, Z.-Y. Wu, Y. Ding, A.-W. Liu, and Q.-S. Zhu, Chem. Phys. Lett. **372**, 659 (2003).
[16] J.-X. Cheng, H. Lin, S.-M. Hu, S.-G. He, Q.-S. Zhu, and A. Kachanov, Appl. Opt. **39**, 2221 (2000).
[17] T. H. Dunning, Jr., J. Chem. Phys. **90**, 1007 (1989).
[18] D. E. Woon and T. H. Dunning, Jr., J. Chem. Phys. **98**, 1358 (1993).
[19] D. E. Woon and T. H. Dunning, Jr., J. Chem. Phys. **103**, 4572 (1995).
[20] J. M. L. Martin and O. Uzan, Chem. Phys. Lett. **282**, 16 (1998).
[21] M. J. Frisch, G. W. Trucks, H. B. Schlegel *et al.*, GAUSSIAN 03, Revision B.4, Gaussian, Inc., Pittsburgh, PA, 2003.
[22] R. W. Davis and M. C. L. Gerry, J. Mol. Spectrosc. **60**, 117 (1976).
[23] A. R. Hoy, I. M. Mills, and G. Strey, Mol. Phys. **24**, 1265 (1972).
[24] J. F. Gaw, A. Willetts, and N. C. Handy, in *Advances in Molecular Vibrations and Collision Dynamics*, edited by J. M. Bowman (JAI, Greenwich, CT, 1990).
[25] I. Mills, *Molecular Spectroscopy: Modern research*, edited by K. N. Rao and C. W. Mathews (Academic, New York, 1972), Vol. 1 p. 115.
[26] I. M. Mills and A. G. Robiette, Mol. Phys. **56**, 743 (1985).
[27] Q.-S. Zhu, H. Qian, H. Ma, and L. Halonen, Chem. Phys. Lett. **177**, 261 (1991).
[28] T. Cours, P. Rosmus, and V. G. Tyuterev, Chem. Phys. Lett. **331**, 317 (2000).
[29] L. Halonen, J. Chem. Phys. **88**, 7599 (1988).
[30] E. B. Wilson, J. C. Decius, and P. C. Cross, *Molecular Vibrations* (Dover, New York, 1980).
[31] D. H. Christensen and O. F. Nielsen, J. Mol. Spectrosc. **27**, 489 (1968).